Supplementary Information

Non-halogenated Solvent Additive Mediated Donor-Acceptor Phase Segregation Leads to Efficient All-Polymer Solar Cells

Yuanxian Liang,[1] Zhenmin Zhao,[1]* Sein Chung,[2] Yuqing Sun,[1] Liang Bai,[1] Jingjing Zhao,[1] Lixing Tan,[1] Kilwon Cho,[2] Zhipeng Kan[1,3]

[1] Center on Nanoenergy Research, Institute of Science and Technology for Carbon Peak & Neutrality, School of Physical Science & Technology, Guangxi University, Nanning 530004, China.

[2] Department of Chemical Engineering, Pohang University of Science and Technology, Pohang 37673, South Korea.

[3] State Key Laboratory of Featured Metal Materials and Life-cycle Safety for Composite Structures, Nanning 530004, China.

* Corresponding author, E-mail: 2007401038@st.gxu.edu.cn

Content

1. Materials

PY-IT, PBQx-TCl, and PDIN were purchased from Solarmer, Inc (Beijing). Carbon disulfide (CS_2) and anisole were purchased from Shanghai Titan Technology Co., Ltd. All materials were used as received without further purification.

2. Methods

OSCs were fabricated in a conventional device configuration of ITO/PEDOT:PSS/ active layers/PDIN/Ag. The glass substrates coated with a layer of indium tin oxide (ITO, 15 Ω/sq) (device area: 0.0361 cm^2). Substrates were prewashed with isopropanol to remove organic residues before immersing in an ultrasonic bath of soap for 15 min. Samples were rinsed in flowing deionized water for 5 min before being sonicated for 15 min each in successive baths of deionized water, acetone, and isopropanol. Next, the samples were dried with pressurized nitrogen before being exposed to an UV-ozone plasma for 15 min. A thin layer of PEDOT:PSS (~30 nm) (CLEVIOSTM P VP AI 4083, Heraeus, Germany) was spin-coated onto the UV-treated substrates, the PEDOT-coated substrates were subsequently annealed on a hot plate at 150 ℃ for 20 min, and the substrates were then transferred into the glovebox for active layer deposition. All solutions were prepared in a nitrogen-filled glovebox using polymer donors (PBQx-TCl) and acceptors (PY-IT). Sequentially, the active layer solution of PBQx-TCl:PY-IT (1:1.3, chloroform, 14 mg/mL，chloroform with CS_2 (1.5% vol) or Anisole(1.5% vol)) was spin-coated at 3000 rpm for 30 s. The CS_2/Anisole was first dissolved in chloroform. After 1 hour of stirring at room temperature, this solution was added to the PBQx-TCl:PY-IT mixture. After stirring overnight, the blend solution was directly spin-coated at 3000 rpm on the PEDOT:PSS treated ITO substrates with thermal annealing treatment at 100 °C for 10 mins. Then a PDIN layer was spin-coated on the active layer as an electron transport layer. Next, the substrates were pumped down in high vacuum at a pressure of 2×10^{-6} Torr, and an Ag layer (100 nm) was thermally evaporated onto the active layer.

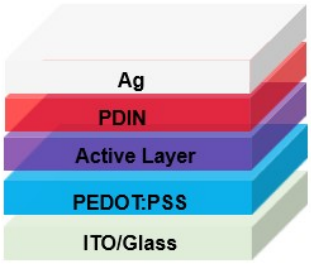

Figure S1. Schematic of the device structure.

3. UV-Vis Absorption

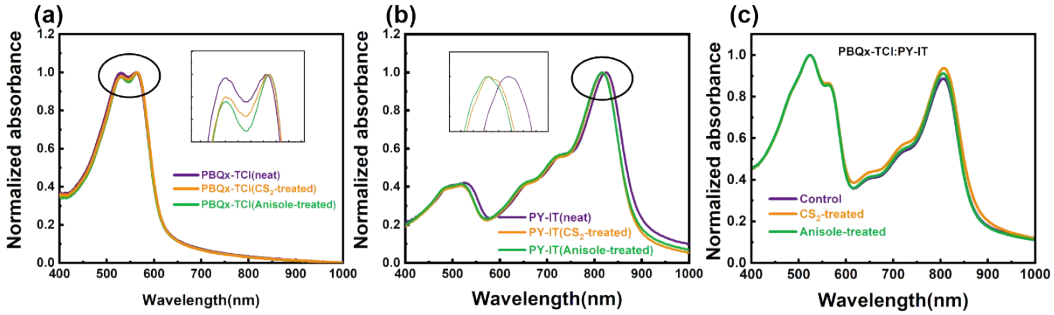

Figure S2. Normalized UV Vis absorption spectra of mixed films of PBQx-TCl: PY-IT systems with different additives, as well as pure films of PBQx-TCl and PY-IT.

4. PL measurements

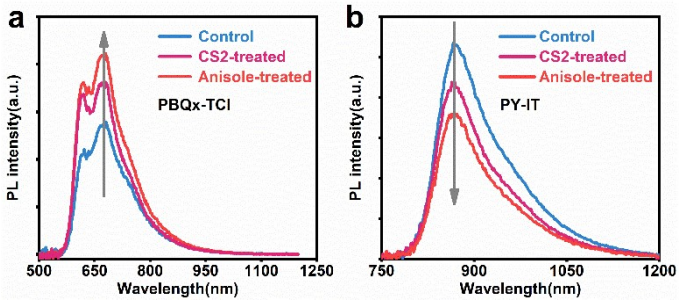

Figure S3. The photoluminescence spectra of **(a)** PBQx-TCl, **(b)** PBQx-TCl with and without additives.

5. Atomic Force Microscopy (AFM) Measurement

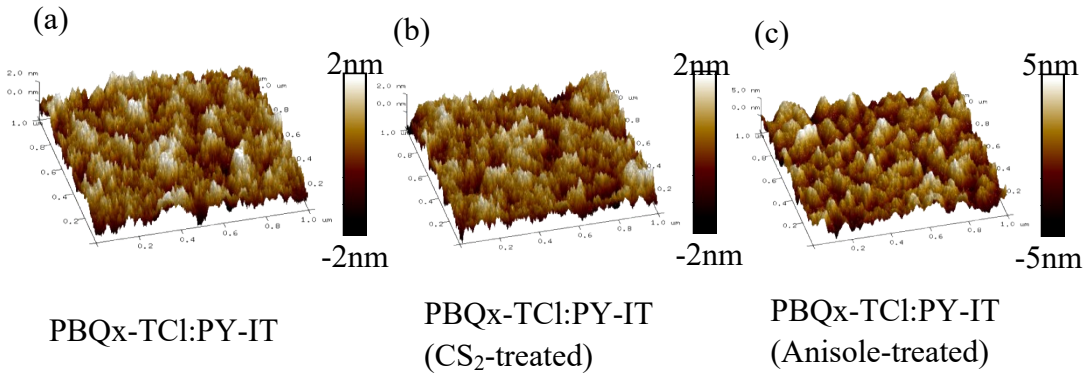

Figure S4. AFM images of PBQx-TCl:PY-IT, PBQx-TCl:PY-IT (CS_2-Treated) and PBQx-TCl:PY-IT (Anisole-Treated).

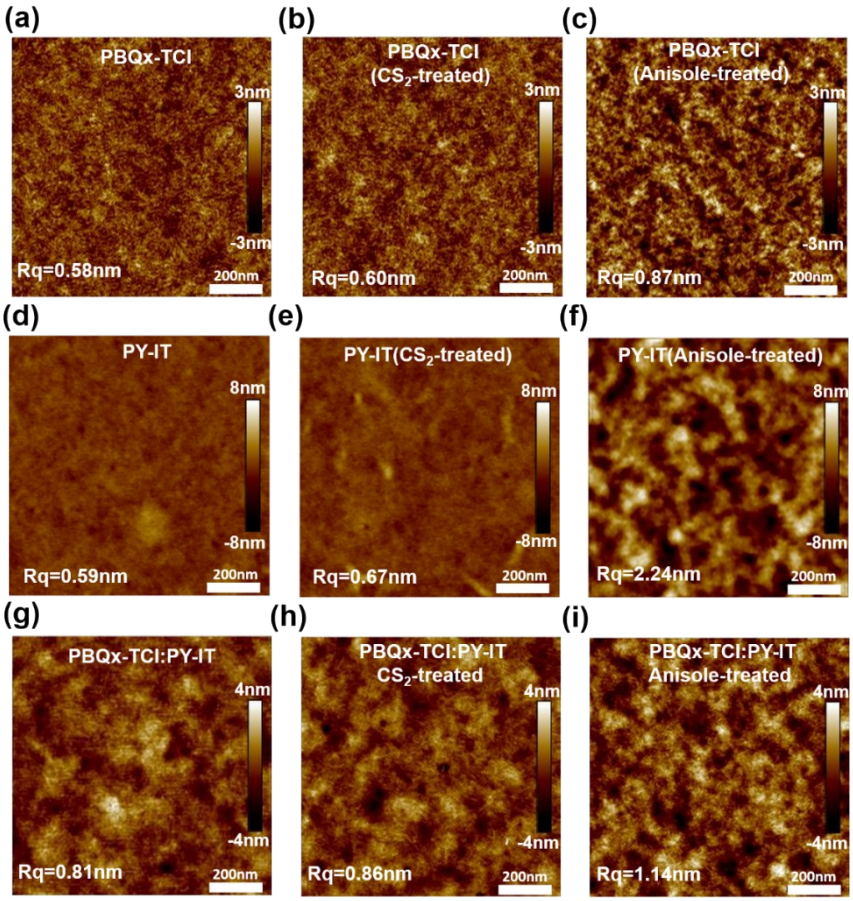

Figure S5. AFM height images of **(a)** as cast PBQx-TCl film, **(b)** CS_2-treated and **(c)** anisole-treated PBQx-TCl films. AFM height images of **(d)** as-cast PY-IT films, **(e)** CS_2-treated and **(f)** anisole-treated PY-IT films. AFM height images of **(g)** as-cast PBQx-TCl:PY-IT film, **(h)** CS_2-treated and **(i)** anisole-treated PBQx-TCl:PY-IT films.

6. Contact Angle

The contact angles of the films were performed on a L2004A1 (Ossila England) contact angle meter. Then the surface free energy was calculated by Owens-Wendt method:

$$\gamma_L \times (1 + cos\theta) = 2 \times (\gamma_L^d \cdot \gamma_{sv}^d)^{\frac{1}{2}} + 2 \times (\gamma_L^p \cdot \gamma_{sv}^p)^{\frac{1}{2}}$$

where and are surface free energy of the probe liquid and sample, respectively, is the contact angle of the sample. The average contact angles of two liquids (deionized water and formamide) on the various neat films were measured and the results (dynamic analysis by video) in Table S5, and the average contact angles and surface energy parameters are summarized in Table 2 (in Manuscript). Then calculate the Flory-Huggins interaction parameter for blend to show the binary miscibility from:

$$K\left(\chi_{donor}^{\frac{1}{2}} - \chi_{acceptor}^{\frac{1}{2}}\right)^2$$

where is the surface energy of the material, K is the proportionality constant. [1,2]

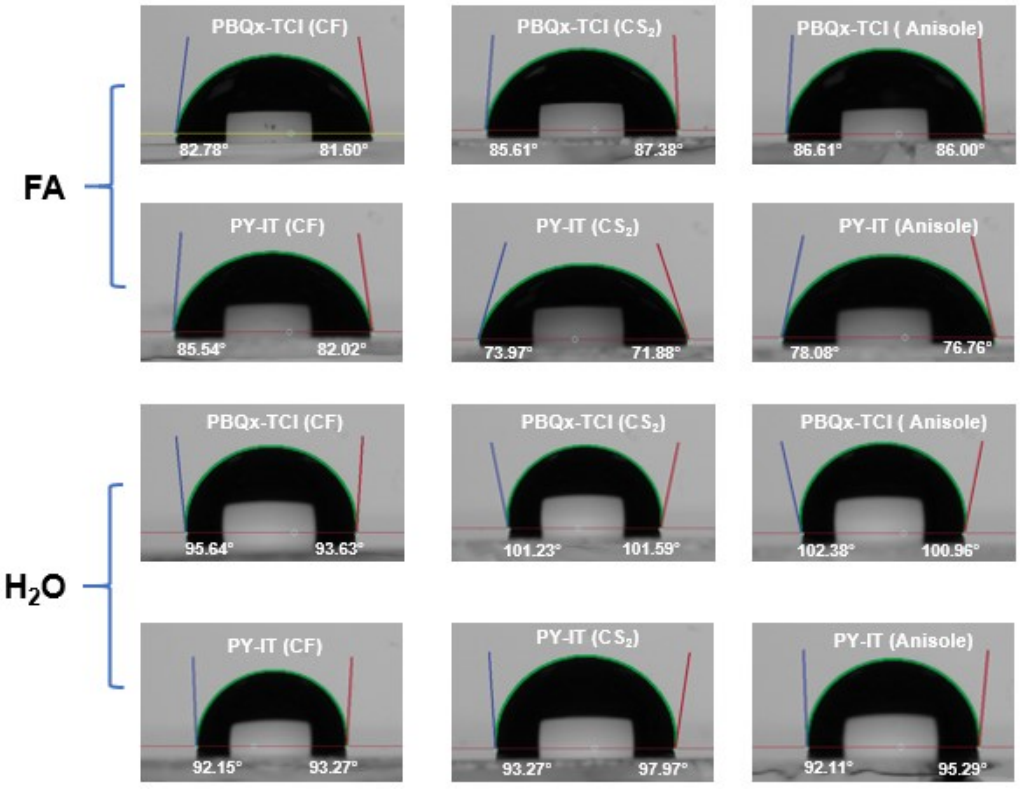

Figure S6. (a) The contact angles of the neat films without additive treatment, with

additive treatment and (b) the additive neat films using deionized water (H2O) and formamide (FA).

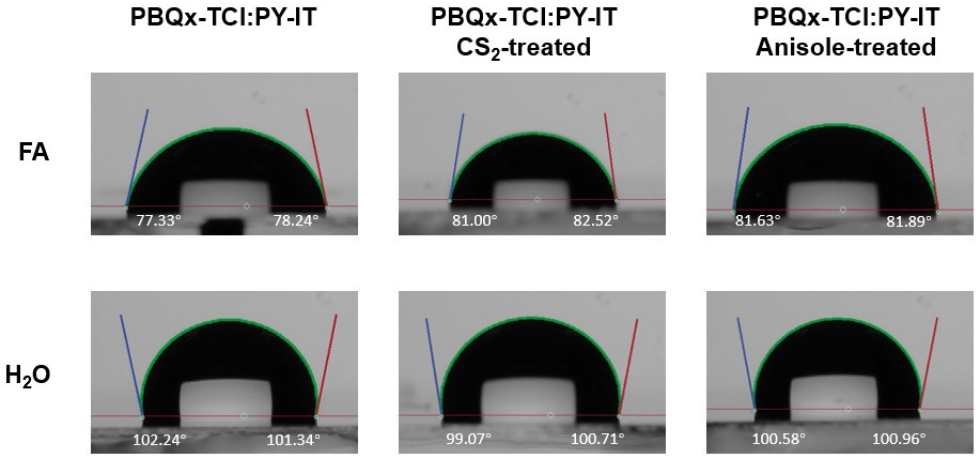

Figure S7. (a) The contact angles of the PBQx-TCl:PY-IT films without additive treatment, with additive treatment and (b) the additive neat films using deionized water (H2O) and formamide (FA).

Table S1. Summarized contact angles of the materials.

Films	Contact angle (deg)			
	H_2O		FA	
PBQx-TCl(Neat)	95.64°	93.63°	82.78°	81.60°
PBQx-TCl(CS_2-treated)	101.23°	101.59°	85.61°	87.38°
PBQx-TCl(Anisole -treated)	102.38°	100.96°	86.61°	86.00°
PY-IT(Neat)	92.15°	93.27°	85.54°	82.02°
PY-IT(CS_2-treated)	93.27°	97.97°	73.97°	71.88°
PY-IT(Anisole-treated)	92.11°	95.29°	78.08°	76.06°
PBQx-TCl :PY-IT(Neat)	102.24°	101.34°	77.33°	78.24°
PBQx-TCl :PY-IT(CS_2-treated)	99.07°	100.71°	81.00°	82.52°
PBQx-TCl:PY-IT(Anisole -treated)	100.58°	100.96°	81.63°	81.89°

Table S2. The surface free energies of PBQx-TCl:PY-IT film without additive treatment with additive treatment were calculated by Owens Wendt method.

PBQx-TCl:PY-IT	Contact angle (deg)	Surface free energy, γ (mJ

Films	H2O (average)	FA (average)	m^{-2})
(Neat)	101.79°	77.78°	26.77
(CS_2-treated)	99.89°	81.73°	20.78
(Anisole -treated)	100.77°	81.76°	21.24

7. Transmission Electron Microscopy (TEM)

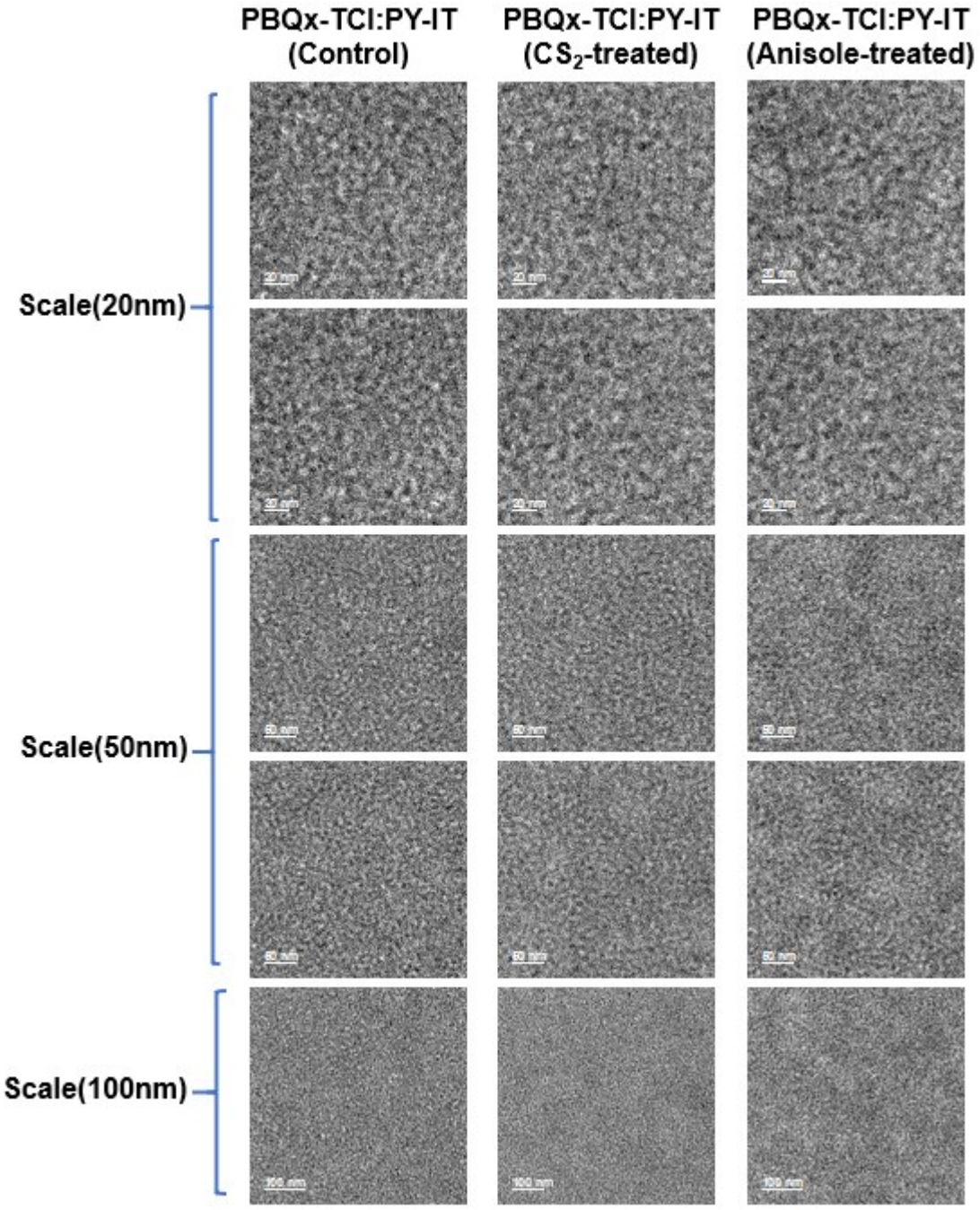

Figure S8. TEM images of the PBQx-TCl:PY-IT active layer at different scales under different conditions.

8. Grazing Incidence Wide-angle X-ray Scattering (GIWAXS)

Table S3. Fitting data obtained from GIWAXS in the in-plane (IP) and out-of-plane (OOP) directions of Control, CS_2-treated and Anisole-treated films of PBQx-TCl.

Conditions	Peak	Peak Location ($Å^{-1}$)	*d*-spacing (Å)	FWHM ($Å^{-1}$)	Crystalline Coherence Length (Å)
PBQx-TCl (Contro)	(IP) (100)	0.30	21.16	0.09	62.1
	(OOP) (010)	1.62	3.88	0.33	16.9
PBQx-TCl (CS_2-treated)	(IP) (100)	0.30	21.01	0.09	62.1
	(OOP) (010)	1.63	3.85	0.33	16.9
PBQx-TCl (Anisole-treated)	(IP) (100)	0.30	21.16	0.09	62.1
	(OOP) (010)	1.62	3.88	0.33	16.9

Table S4. Fitting data obtained from GIWAXS in the in-plane (IP) and out-of-plane (OOP) directions of Control, CS2-treated and Anisole-treated films of PY-IT.

Conditions	Peak	Peak Location ($Å^{-1}$)	*d*-spacing (Å)	FWHM ($Å^{-1}$)	Crystalline Coherence Length (Å)
PY-IT (Control)	(IP) (100)	0.35	17.75	0.14	39.9
	(OOP) (010)	1.61	3.90	0.32	17.5
PY-IT (CS_2-treated)	(IP) (100)	0.35	17.75	0.14	39.9
	(OOP) (010)	1.62	3.88	0.29	19.3
PY-IT (Anisole-treated)	(IP) (100)	0.35	17.85	0.14	39.9
	(OOP) (010)	1.61	3.90	0.27	20.7

Table S5. Fitting data obtained from GIWAXS in the in-plane (IP) and out-of-plane (OOP) directions of Control, CS_2-treated and Anisole-treated films of PY-IT.

Conditions	Peak	Peak Location ($Å^{-1}$)	*d*-spacing (Å)	FWHM ($Å^{-1}$)	Crystalline Coherence Length (Å)
PBQx-TCl:PY-IT (Control)	(IP) (100)	0.31	20.01	0.14	39.9
	(OOP) (010)	1.62	3.88	0.33	16.9
PBQx-TCl:PY-IT (CS_2-treated)	(IP) (100)	0.31	20.20	0.13	43.0
	(OOP) (010)	1.61	3.90	0.31	18.0
PBQx-TCl:PY-IT (Anisole-treated)	(IP) (100)	0.31	20.20	0.13	43.0
	(OOP) (010)	1.62	3.88	0.29	19.3

9. Device Characterization

The J−V measurement was performed via a XES-50S1 (SAN-EI Electric Co., Ltd.) solar simulator (AAA grade) whose intensity was calibrated by a certified standard silicon solar cell (SRC-2020, Enlitech) under illumination of AM 1.5G 100 mW cm−2. The AM 1.5G light source with a spectral mismatch factor of 1.01 was calibrated by the National Institute of Metrology. The intensity of the AM 1.5G spectra was calibrated by a certified standard silicon solar cell (SRC-2020, Enlitech) calibrated by the National Institute of Metrology. The J-V curves of small-area devices were measured in forwarding scan mode (from -0.2 V to 1.2 V) with a scan step length of 0.02 V. The external quantum efficiency (EQE) was measured by a certified incident photon to electron conversion (IPCE) equipment (QE-R) from Enli Technology Co., Lt. The light intensity at each wavelength was calibrated using a standard monocrystalline Si photovoltaic cell.

For TPV, the measurement was conducted under 1 sun conditions by illuminating the device with a white light-emitting diode, and the champion device is set to the open-circuit condition. For TPC, the champion device is set to the short-circuit condition in dark. The output signal was collected by key sight oscilloscope. The transient photocurrent (TPC) was testing under the short-circuit condition to explore the time-dependent extraction of photogenerated charge carriers. The 10 ns light plus laser were selected to the light source for steady the photogenerated current density. The devices are otherwise kept in the dark between pulses in order to avoid any influence of pulse frequency on the current responses. The transient photovoltage (TPV) was testing under the open-circuit condition to explore the photovoltage decay.

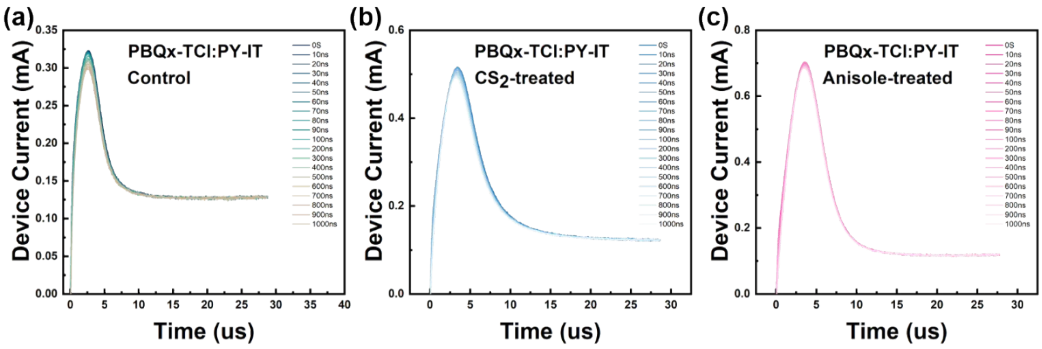

Figure S9. The current transients of (a) Control, (b) CS2-treated and (c) Anisole-treated.

Table S6. Detailed device parameters of solar cells from the PBQx-TCl:PY-IT system with different amounts of Anisole.

Anisole content	V_{OC} (mV)	J_{SC} (mA cm^{-1})	FF (%)	PCE$_{max}$ (%)	Ave.PCE (%)
0 vol%	0.965	24.45	68.1	16.2	16.1
1 vol%	0.966	24.59	70.7	16.8	16.7
1.5 vol%	0.964	24.91	71.9	17.3	17.0
2 vol%	0.963	24.84	70.82	16.95	16.6

Table S7. Detailed device parameters of solar cells from the PBQx-TCl:PY-IT system with different amounts of CS_2.

Anisole content	V_{OC} (mV)	J_{SC} (mA cm^{-1})	FF (%)	PCE$_{max}$ (%)	Ave.PCE (%)
0 vol%	0.965	24.45	68.1	16.2	16.1
1 vol%	0.960	25.22	68.8	16.7	16.6
1.5 vol%	0.959	25.6	69.4	17.0	16.9
2 vol%	0.957	25.4	68.8	16.7	16.6

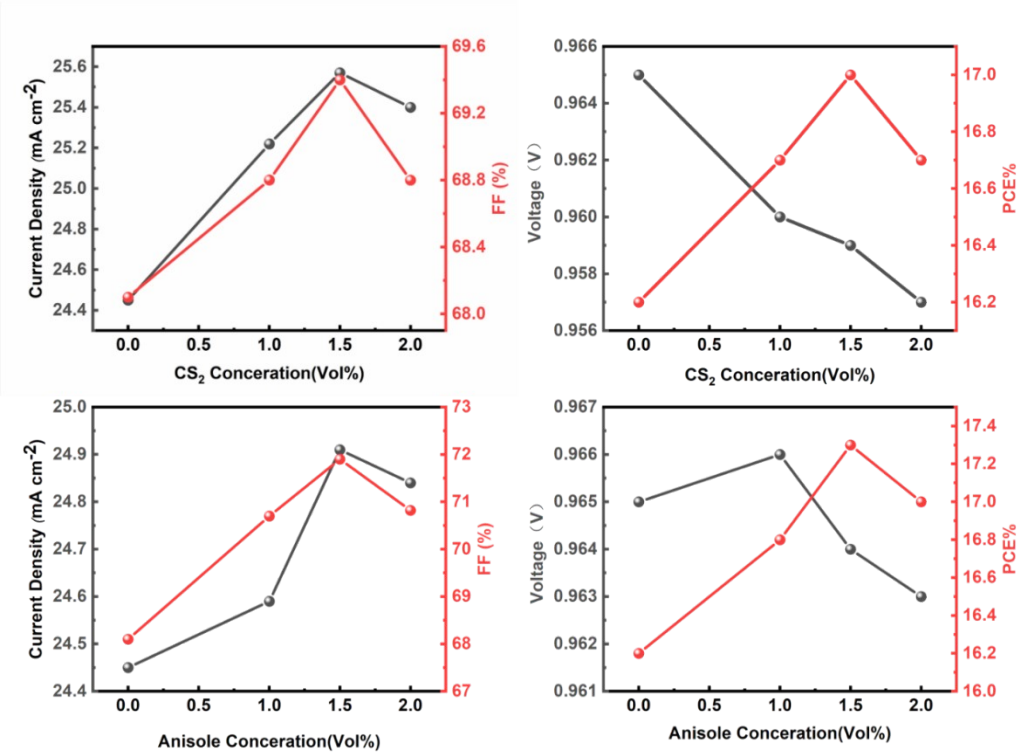

Figure S10. Photovoltaic performances of PM6:PY-IT based OSCs with different concentrations of CS2 and Anisole.

10. Carrier Extraction by Linearly Increasing Voltage (CELIV)

According to Mozer et al.'s recombination model, carrier density n(t) over time can be expressed as: [3,4]

$$n(t) = \frac{n_0}{1 + \left(\frac{t}{\tau_b}\right)^{\gamma}}$$

where n(t) is the charge density at time t, n_0 is the initial charge density, τ_b is the recombination lifetime, and γ is the dispersion parameter. According to ref. γ =1 for trap-free bimolecular recombination and is <1 for the dispersive bimolecular recombination. In the dispersive bimolecular recombination, the decay of carrier density is given by:

$$\beta(t) = -\frac{\frac{dn(t)}{d(t)}}{n^2(t)}$$

where n(t) is the carrier density and $\beta(t)$ is dispersive bimolecular recombination rate at a delay time t. Substituting the first equation, the bimolecular recombination rate $\beta(t)$ can also be expressed as:

$$\beta(t) = (\frac{1}{\tau_b})\gamma {n_0}^{-1}(\frac{t}{\tau_b})^{\gamma-1}$$

The resulting $\beta(t)$ can be calculated from the fitting parameters n(0), τ_b and γ using equation above.[5]

11. References

1. Z. Cao, J. Chen, S. Liu, M. Qin, T. Jia, J. Zhao, Q. Li, L. Ying, Y.-P. Cai, X. Lu, F. Huang and Y. Cao, Chem. Mater., 2019, **31**, 8533-8542.
2. S. Pang, R. Zhang, C. Duan, S. Zhang, X. Gu, X. Liu, F. Huang and Y. Cao, Adv. Energy Mater., 2019, **9**, 1901740.
3. A. Pivrikas, G. Ju š ka, A. J. Mozer, M. Scharber, K. Arlauskas, N. S. Sariciftci, H. Stubb, R. Österbacka., Physical Review Letters, 2005, **94**, 177801.
4. A. J. Mozer, G. Dennler, N. S. Sariciftci, M. Westerling, A. Pivrikas, R. Österbacka, G. Juška., Physical Review B, 2005, **72**, 035217.
5. Y. Liu, Y. Gao, B. Xu, P. H. M. van Loosdrecht, W. Tian., Organic Electronics, 2016, **38**, 8-14.